

TDC Offset Estimation from Motored Cylinder Pressure Data based on Heat Release Shaping

P. Tunestål

Dept. of Energy Sciences, Lund University, P.O. Box 118, 221 00 Lund - Sweden
e-mail: per.tunestal@energy.lth.se

Résumé — Estimation du décalage de PMH à partir de données de pression de cylindre moteur basées sur la conformation de libération de chaleur

— La détermination du décalage de Point Mort Haut (PMH) correct d'un moteur à combustion interne est plus difficile qu'il n'y paraît. Cette étude introduit une nouvelle méthode destinée à déterminer le décalage de PMH sur la base de la simple supposition que la puissance de perte de chaleur à travers les parois de la chambre de combustion soit constante pour des cycles moteur selon un intervalle d'angle de bras de manivelle étroit autour du PMH. La méthode proposée utilise une optimisation des moindres carrés non linéaire pour déterminer la combinaison de rapport de chaleur spécifique et de décalage de PMH qui rend la puissance de perte de chaleur aussi constante que possible. Un sous-problème important consiste à déterminer la localisation de pression de pic avec une haute précision. L'application d'une série de Fourier du troisième ordre à la pression de cylindre moteur permet l'estimation du maximum de pression moyennant un écart-type de $0,005^\circ$ d'angle de bras de manivelle (AM) et elle peut être également utilisée à la place de la pression mesurée afin de réduire l'incertitude de l'estimation du PMH d'environ 50 %. L'écart-type d'une estimation de PMH de cycle unique est approximativement de $0,025^\circ$ d'AM lors de l'utilisation d'une résolution de bras de manivelle de $0,2^\circ$ d'AM pour les mesures. L'erreur systématique de l'estimation de PMH se situe dans la plage allant de 0 à $0,02^\circ$ d'AM par comparaison à la fois avec les mesures réalisées au moyen d'un détecteur de PMH et avec des cycles moteur simulés. La méthode peut être utilisée à la fois à des fins d'étalonnage et de diagnostics à bord, par exemple pendant un démarrage, une coupure de carburant ou un arrêt du moteur. La série de Fourier du troisième ordre appliquée s'accompagne d'une pénalisation de calcul significative mais, puisqu'elle n'est appliquée que de façon très intermittente, ceci ne doit pas poser un problème sérieux.

Abstract — TDC Offset Estimation from Motored Cylinder Pressure Data based on Heat Release Shaping

— Finding the correct Top Dead Center (TDC) offset for an internal combustion engine is harder than it seems. This study introduces a novel method to find the TDC offset based on the simple assumption that the heat loss power through the combustion chamber walls is constant for motored cycles in a narrow Crank Angle interval around TDC. The proposed method uses nonlinear least squares optimization to find the combination of specific heat ratio and TDC offset that makes the heat loss power as constant as possible. An important subproblem is to determine the peak pressure location with high accuracy. Fitting a third order Fourier series to the motored cylinder pressure allows the pressure maximum to be estimated with a standard deviation of 0.005° Crank Angle (CA) and it can also be used instead of the measured pressure to reduce the uncertainty of the TDC estimate by approximately 50%. The standard deviation of a single-cycle TDC estimate is approximately 0.025° CA when using a crank resolution of 0.2° CA for the measurements. The bias of the TDC estimate is in the $0-0.02^\circ$ CA range both when comparing to measurements with a TDC sensor and with simulated

motored cycles. The method can be used both for calibration and on-board diagnostics purposes e.g. during cranking, fuel cut-off or engine switch-off. The third order Fourier series fit comes with a significant computational penalty but since it is only applied very intermittently this does not have to be a serious issue.

NOMENCLATURE

a	Crank radius
α	Crank Angle
B	Cylinder bore diameter
CA	Crank Angle
$^{\circ}$ CA	Crank Angle (in degrees after TDC)
C_p	Molar specific heat at constant pressure
C_v	Molar specific heat at constant volume
γ	Specific heat ratio
dQ	Incremental heat transfer
dU	Incremental change of internal energy
dW	Incremental work
ϵ	Residual between model and measurement
E	Residual vector
φ	Regressor vector for LLS problem
Φ	Regressor matrix for LLS problem
GETDC	Gas Exchange Top Dead Center
l	Connecting rod length
LLS	Linear Least Squares
n	Number of moles
NLLS	NonLinear Least Squares
p	Pressure
R	Universal gas constant (molar representation)
dT	Incremental change of temperature
TDC	Top Dead Center
θ	Parameter vector for least squares problem
V	Volume
V_c	Clearance volume
y	Output variable for LLS problem
Y	Output vector for LLS problem

INTRODUCTION

All modern internal combustion engines are equipped with some kind of crank position sensor. Production engines usually have a toothed flywheel with an inductive sensor that can sense when one of the teeth is in the vicinity of the sensor. In this way the engine controller can keep track of the crank position of the engine. In a laboratory setting the crank position sensor would more likely consist of an optical encoder with very high resolution (1 800-3 600 pulses per revolution). Both sensor types can provide differential crank position information quite accurately but the absolute Crank Angle (CA) has to be meticulously calibrated.

Accurate calibration of the absolute crank position is extremely important since it has a very strong influence on the calculation of e.g. Indicated Mean Effective Pressure

(IMEP) and heat release. In Reference [1], it is concluded that the IMEP error from incorrect Crank Angle phasing is between 3 and 10% per degree, and thus to ensure an error below 1% the Crank Angle phasing has to be correct to within 0.1° CA.

The calibration of Crank Angle phasing can be performed by checking the sensor output when the piston is at Top Dead Center (TDC). This method gives, at best, an accuracy corresponding to the resolution of the crank position sensor. A further complicating factor is that it is very hard to determine exactly when the piston is at TDC since the crank position has, by definition, no influence on the piston position at TDC. In some cases it is possible to improve the accuracy by determining the two crank positions when the piston has travelled a specific (small) distance from TDC and then deduce that TDC is at the crank position in the middle between these two positions.

Another way of calibrating the crank position sensor is by measuring the motored cylinder pressure of the engine and finding the crank position of peak cylinder pressure. According to experience the peak cylinder pressure for a normal internal combustion engine always appears around $0.3-0.5^{\circ}$ CA before TDC. This distance between the peak cylinder pressure and TDC is sometimes called the thermodynamic loss angle. As described in Reference [2] the $\log p - \log V$ diagram should show straight lines for the compression and expansion strokes respectively. This requirement can be used to pin down the exact TDC position.

There are also more sophisticated methods to find the correct TDC position. In Reference [3], a method is proposed that uses the fact that an incorrect TDC introduces a non-physical loop in the temperature-entropy diagram. The TDC position is adjusted until the loop disappears and then an additional 0.45° CA correction is added. This additional correction was found necessary from simulations. The weak points with this method are that it requires the calculation of gas temperature which is often inaccurate. The calculated temperature is then used both directly and in entropy polynomials.

Another method proposed by [4] explores symmetries at the inflexion points of the pressure trace during compression and expansion respectively. The method relies on second derivatives of both pressure and volume which makes it very sensitive to measurement noise however. In Reference [5] the method is refined and it is concluded that the Vdp term must have an inflexion point at the Crank Angle of maximum pressure. This can be used to find the correct TDC

position. The drawback with the method is that it requires third derivatives of measured cylinder pressure which makes it extremely sensitive to noise. A zero phase-lag smoothing is applied to get around this problem and average TDC estimates based on 20-30 cycles show a variability of only $\pm 0.02^\circ$ CA.

In Reference [6], an attempt is made to identify all parameters necessary for heat release calculation from cylinder pressure measurements alone. This is done by minimizing the difference between measured and simulated cylinder pressure over a large Crank Angle interval. An optimal value for the TDC position was obtained using this method but it varied by as much as 0.5° CA between different operating points. One explanation is that a TDC position error has little influence on the cylinder pressure far away from TDC and thus a small estimation interval is favorable. A closely related method is the one described in Reference [7] where the asymmetry of the pressure trace around TDC is analysed using thermodynamic cycle simulation. The TDC position is adjusted until the asymmetry between two arbitrary points in the compression and expansion strokes respectively is correctly reproduced. The method gives the correct TDC position to within approximately 0.05° CA. In Reference [8], another method based on symmetry/asymmetry of the pressure trace is developed and compared to four existing methods of varying complexity. The method is fairly accurate and robust but requires knowledge of the polytropic exponent which has to be established through simulations.

Attempts to determine the TDC position dynamically for firing cycles have also been made. Reference [9] derives some necessary conditions for the polytropic exponent that can be used to correct the TDC position. The method provides a TDC correction that varies by approximately 0.5° CA which is usually not accurate enough.

Considering the inaccuracies of the present TDC calibration methods as well as the awkwardness of having to take the engine apart in order to find the correct TDC location, an accurate non-intrusive method would be most desirable. This paper develops a method for TDC calibration based on motored cylinder pressure data. The method relies on a simple thermodynamic model of the gas in the combustion chamber in the vicinity of TDC. In addition to TDC position, the method also estimates heat transfer and specific heat ratio and thus only geometric details are required as prior knowledge. The presented method is suitable both for calibration and on-board diagnostics purposes. On board the method can be applied whenever there is no combustion, *e.g.* during cranking, fuel cut-off or engine switch-off.

A large part of the information in this paper was previously published by the author in [10]. This paper, however, improves the TDC offset estimation by using a fitted third order Fourier series representation of the motored cylinder pressure instead of the raw measurements. The high quality of the fit removes some of the noise problems associated

with numerical differentiation as well as locating the maximum pressure and thus reduces the standard deviation of the TDC offset estimate.

1 THERMODYNAMIC MODEL

The combustion chamber of an internal combustion engine can be modeled as a closed thermodynamic system that interacts with its environment through work and heat only. It is here assumed that the mass transfer is either negligible or that its effects on the pressure can be accurately modeled as an equivalent heat interaction. Given these assumptions, the change in internal energy during a thermodynamic process can be written as:

$$dU = dQ - dW \quad (1)$$

where dU , dQ and dW represent change in internal energy, heat transfer to the system and work performed by the system respectively. The differentials in Equation (1) simplify the notation somewhat although it should be kept in mind that they really represent time derivatives or, more commonly, Crank Angle derivatives. The Crank Angle derivatives are convenient since there is a one-to-one correspondence between Crank Angle and combustion chamber volume. This can be understood from Figure 1. With the geometry of Figure 1, the instantaneous combustion chamber volume is given by:

$$V(\alpha) = V_c + \frac{\pi B^2}{4} [l + a(1 - \cos(\alpha)) - (l^2 - a^2 \sin^2(\alpha))^{1/2}] \quad (2)$$

It should be noted here that Equation (2) assumes a cylinder without pin offset *i.e.* that the center of the piston pin is located exactly above the center of the crank shaft. This is true for most engines but the expression for the instantaneous combustion chamber volume can easily be adjusted to include a pin offset.

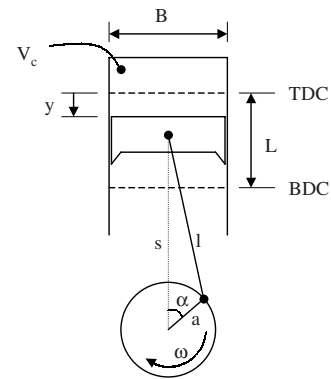


Figure 1

Crank geometry of a combustion engine cylinder.

If it is further assumed that there are no chemical reactions and that the specific heat is constant, the change in internal energy can also be written as:

$$dU = nC_v dT - pdV = \frac{C_v}{R} d(pV) \quad (3)$$

where n represents the number of moles in the combustion chamber and C_v represents the molar specific heat. Note that molar representation is selected throughout the paper. Combining (1) with (3) and rewriting the work term to include only reversible work an expression for dQ can be obtained.

$$\begin{aligned} dQ &= dU + dW = \frac{C_v}{R} d(pV) + pdV \\ &= \frac{C_v + R}{R} pdV + \frac{C_v}{R} Vdp \end{aligned} \quad (4)$$

Using the fact that $C_p - C_v = R$ for an ideal gas and the definition of specific heat ratio, γ , Equation (4) can be rewritten as:

$$\begin{aligned} dQ &= \frac{C_p}{C_p - C_v} pdV + \frac{C_v}{C_p - C_v} Vdp \\ &= \frac{\frac{C_p}{C_v}}{\frac{C_p}{C_v} - \frac{C_v}{C_v}} pdV + \frac{\frac{C_v}{C_v}}{\frac{C_p}{C_v} - \frac{C_v}{C_v}} Vdp \\ &= \frac{\gamma}{\gamma - 1} pdV + \frac{1}{\gamma - 1} Vdp \end{aligned} \quad (5)$$

which is the well known differential equation for calculating apparent heat release.

2 TDC OFFSET ESTIMATION

The instantaneous volume of the combustion chamber is specified by the Crank Angle using Equation (2). As mentioned above, the relative Crank Angle can be accurately measured whereas its absolute value (the TDC offset) is regarded as unknown. The relative cylinder pressure can also be accurately measured whereas the absolute level has to be determined by pressure pegging. The specific heat ratio can either be determined from the gas composition and temperature or it can be treated as an unknown. The latter approach is taken in this text.

2.1 Theory

The estimation method developed in this text utilizes the fact that the temperature and pressure is fairly constant in the vicinity of TDC. It is further assumed that the wall temperature and the in-cylinder flow are essentially constant. All these assumptions together imply that the heat transfer, dQ/dt , is constant. With the additional assumption that the angular velocity of the crank shaft is constant, it follows that $dQ/d\alpha$, where α denotes Crank Angle, is constant.

The model, (5), can be rewritten on a form suitable for parameter estimation.

$$\frac{dp}{d\alpha} = (\gamma - 1)k \frac{1}{V(\alpha)} - \gamma p(\alpha) \frac{dV/d\alpha}{V(\alpha)} \quad (6)$$

where k represents the constant heat gain per Crank Angle. In Equation (6) the explicit dependence on Crank Angle has been emphasized in order to avoid misunderstandings.

The final thing to include in the model is the actual Crank Angle offset (TDC offset). This is done by adding an offset, α_0 to the Crank Angle argument of the cylinder pressure.

$$\begin{aligned} \frac{dp}{d\alpha}(\alpha + \alpha_0) &= (\gamma - 1)k \frac{1}{V(\alpha)} \\ &\quad - \gamma p(\alpha + \alpha_0) \frac{dV/d\alpha}{V(\alpha)} \end{aligned} \quad (7)$$

The reason for not including the offset in the Crank Angle argument for the volume is that the offset represents the difference in phasing between the pressure measurements and the corresponding volume trace. The reason for not including the offset in the Crank Angle argument for the volume is that the volume is a known function of the true Crank Angle and has nothing to do with the unknown Crank Angle offset in the Crank Angle measurements.

Estimation of the TDC offset is based on Equation (7) which contains three unknown parameters.

$$\theta = \begin{pmatrix} k_1 \\ \gamma \\ \alpha_0 \end{pmatrix} \quad (8)$$

In Equation (8), $k_1 = (\gamma - 1)k$ has been used as parameter. In general, the equality in Equation (7) will not hold and thus a residual is defined by:

$$\begin{aligned} \epsilon(\alpha; \theta) &= \frac{dp}{d\alpha}(\alpha + \alpha_0) - (\gamma - 1)k \frac{1}{V(\alpha)} \\ &\quad + \gamma p(\alpha + \alpha_0) \frac{dV/d\alpha}{V(\alpha)} \end{aligned} \quad (9)$$

Given a sequence $\alpha_1 \dots \alpha_n$ of consecutive Crank Angle measurements around TDC, a residual vector can be defined as:

$$E(\theta) = \begin{pmatrix} \epsilon(\alpha_1; \theta) \\ \vdots \\ \epsilon(\alpha_n; \theta) \end{pmatrix} \quad (10)$$

The best set of parameters can now be found by solving the nonlinear least squares (NLLS) problem:

$$\hat{\theta} = \arg \min_{\theta} \|E(\theta)\|_2 \quad (11)$$

It is subsequently noted that the dependence in (9) on the first two parameters is linear whereas the dependence on the last parameter is nonlinear. This can be utilized in a similar

manner as in [11] where a nonlinear least squares problem is separated into one Linear Least Squares (LLS) problem and one NLLS problem. For this purpose the parameter vector in (8) is divided into one linear, θ_l and one nonlinear part, θ_{nl} .

$$\theta = \begin{pmatrix} \theta_l \\ \theta_{nl} \end{pmatrix} \quad (12)$$

where

$$\theta_l = \begin{pmatrix} k_1 \\ \gamma \end{pmatrix} \quad (13)$$

$$\theta_{nl} = \alpha_0 \quad (14)$$

The output, y , and regressor vector, φ , for the LLS problem are respectively defined by:

$$y(\alpha; \theta_{nl}) = \frac{dp}{d\alpha}(\alpha + \alpha_0) \quad (15)$$

and

$$\varphi = \begin{pmatrix} 1 \\ V(\alpha) \\ p(\alpha + \alpha_0) \frac{dV/d\alpha}{V(\alpha)} \end{pmatrix} \quad (16)$$

The equation on standard form used for the LLS problem is thus given by:

$$y(\alpha; \theta_{nl}) = \varphi\theta_l \quad (17)$$

Output vector and regressor matrix are constructed according to:

$$Y(\theta_{nl}) = \begin{pmatrix} y(\alpha_1; \theta_{nl}) \\ \vdots \\ y(\alpha_n; \theta_{nl}) \end{pmatrix} \quad (18)$$

$$\Phi = \begin{pmatrix} \varphi(\alpha_1) \\ \vdots \\ \varphi(\alpha_n) \end{pmatrix} \quad (19)$$

The standard linear least squares solution is then given by:

$$\hat{\theta}_l(\theta_{nl}) = (\Phi^T \Phi)^{-1} \Phi^T Y(\theta_{nl}) \quad (20)$$

The solution to the original NLLS problem, (11), can now be stated as:

$$\begin{aligned} \hat{\theta} &= \arg \min_{\theta} \|E(\theta)\|_2 \\ &= \arg \min_{\theta_{nl}} \|E(\theta_{nl}; \hat{\theta}_l(\theta_{nl}))\|_2 \end{aligned} \quad (21)$$

The separation of the NLLS problem into a linear and a nonlinear part has thus reduced the NLLS problem into estimation of only one parameter, the TDC offset. Due to the nature of the problem, the residual norm has a very regular dependence on the TDC offset. A representative example of the residual norm dependence on TDC offset for one cycle is shown in Figure 2. A simple Newton method *e.g.* as described in [12] should be able to find the optimum in

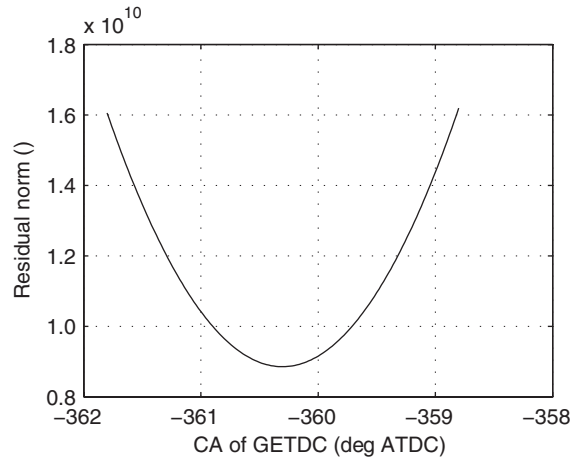


Figure 2
Residual norm dependence on TDC offset.

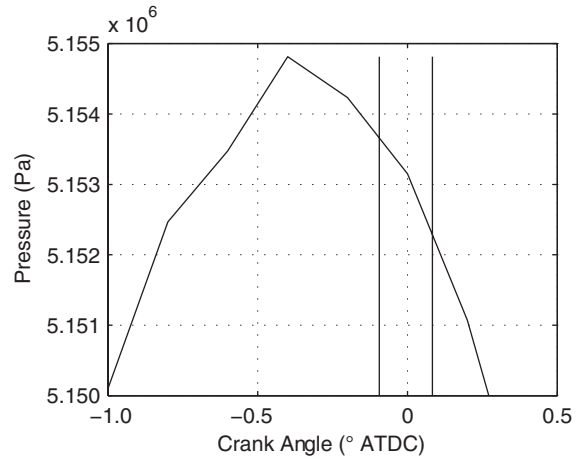


Figure 3
95% confidence interval of TDC estimate based on a single cycle for simulated motored pressure. Pressure trace in figure represents ensemble average of 100 cycles.

just a few iterations. Figure 3 shows the 95% confidence interval for a TDC estimate based on a single simulated cycle together with the ensemble average of the pressure trace based on 100 cycles. The simulated pressure trace was generated with realistic models for both specific heat ratio and heat transfer and white noise of realistic amplitude was added. With the suggested estimation interval an estimator with a bias of 0.01° CA and a standard deviation of 0.05° CA is obtained.

Although the estimates of specific heat ratio and heat power are merely side effects it is interesting to see their actual values. For the same simulated cycles as above the specific heat ratio estimate is 1.35 and the heat power

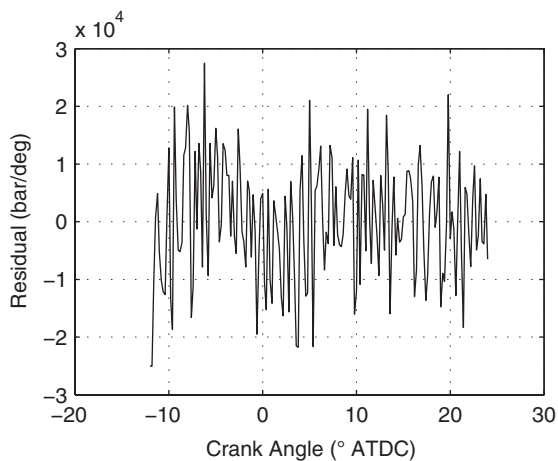


Figure 4
Residual with optimal TDC.

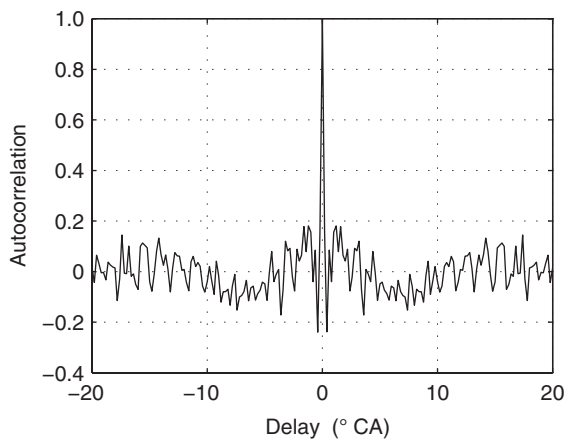


Figure 5
Autocorrelation of residual vector with optimal TDC.

is $-3.6 \text{ J/}^\circ \text{ CA}$ which are reasonable values for motored cycles without fuel injection. A typical optimal residual vector is shown as a function of Crank Angle in Figure 4. No clear trends can be seen in the residual which indicates that the selected model structure is sufficient to describe the real behavior. The autocorrelation of the residual, shown in Figure 5, confirms that the residual is an essentially uncorrelated sequence.

2.2 Selection of Estimation Interval

Application of the TDC estimation method above requires selection of a suitable Crank Angle interval for the estimation to be based on. A long estimation interval with a large number of measurements is desirable in order to reduce the influence of measurement noise on the estimate. On the

other hand, the assumption of constant heat transfer rate and specific heat ratio is more valid for a short estimation interval. Thus a compromise is necessary between good statistics and fidelity of the model.

When applying the estimation method to simulated motored pressure traces it turns out that a suitable estimation interval is $[-12, 24]^\circ \text{ CA}$. The relatively large asymmetry with respect to TDC is somewhat surprising.

2.3 Finite Crank Sensor Resolution

Since pressure measurements from a combustion engine are normally taken at fixed Crank Angles dictated by the crank position sensor, and this sensor has limited resolution, it is most convenient (and least error prone) to maintain the same set of pressure measurements throughout the optimization. This means that the estimation interval will actually move around somewhat (in Crank Angle space) with the changing Crank Angle offset. This does not quite correspond to the ideal representation in Equations (6–21) but the influence will be very small as long as the initial estimate is close to the real Crank Angle offset. This is ensured by selecting the initial TDC position as the maximum pressure position corrected for a nominal loss angle which is normally in the range $0.3\text{--}0.6^\circ \text{ CA}$.

2.4 Maximum Pressure Position

Finding the correct maximum pressure position is not as straightforward as it seems when noisy pressure measurements are considered. The sample with the maximum pressure value could be as much as 1° CA from the thermodynamically correct Crank Angle of maximum pressure. This means that some kind of interpolation or curve fitting has to be applied in order to obtain better accuracy.

The most straightforward solution is to fit a second order polynomial to the pressure samples surrounding the sample with the maximum value but it turns out that the motored cylinder pressure is only well described by a second order polynomial within a few Crank Angle degrees from the maximum. A curve fit based on so few samples does not offer much improvement compared to just picking the position of the sample with the highest pressure value.

Since the motored cylinder pressure resembles a sinusoidal a low order Fourier series could be considered. It turns out that a third order Fourier series provides an almost perfect fit over a wide enough Crank Angle interval in order to provide good statistics for the curve fit. An example of a third order Fourier series fit to a single motored cylinder pressure trace in the interval $[-13, 25]^\circ \text{ CA}$ is shown in Figure 6 and the residuals are shown in Figure 7. Figure 8 shows estimated maximum pressure locations from 1000 simulated motored pressure traces with a noise standard deviation of 2 kPa which corresponds to the level of real measurement noise. The resulting standard deviation of

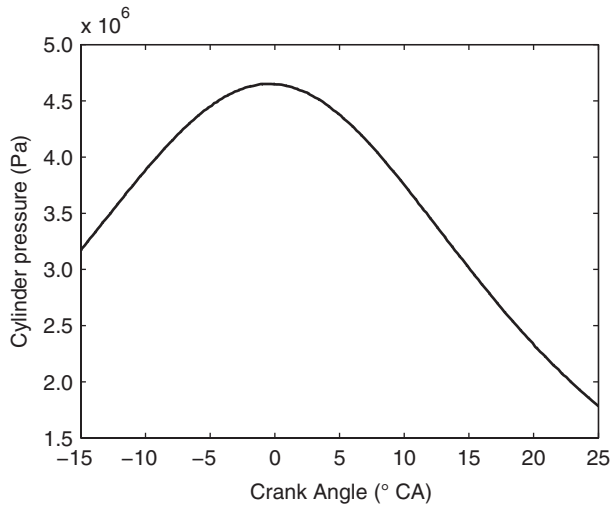


Figure 6

Third order Fourier series fit to motored cylinder pressure. The (invisible) dashed line represents measured cylinder pressure whereas the solid line represents the Fourier series fit.

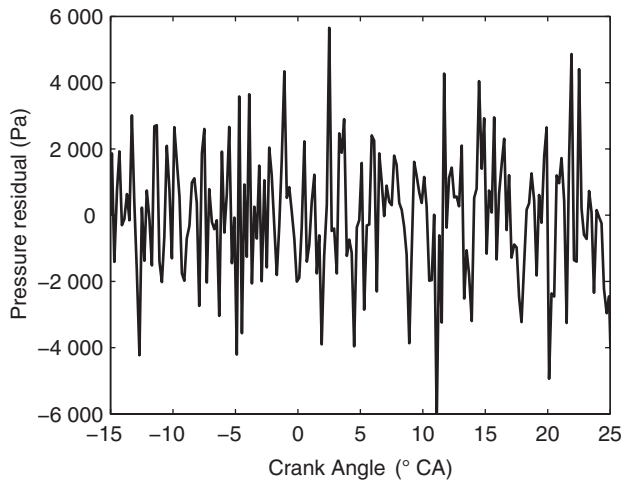


Figure 7

Residuals from the third order Fourier fit to a motored cylinder pressure trace.

single-cycle estimates of the maximum pressure location is 0.006° CA which is more than adequate. If the noise level is doubled the standard deviation of the estimate is approximately tripled. Evenso, the uncertainty is still quite acceptable and it can be concluded that a third order Fourier fit is suitable for finding the correct Crank Angle of the maximum pressure.

2.5 Uncertain Absolute Pressure Level

Another practical concern is the absolute pressure level. Most pressure sensors suitable for cylinder pressure sens-

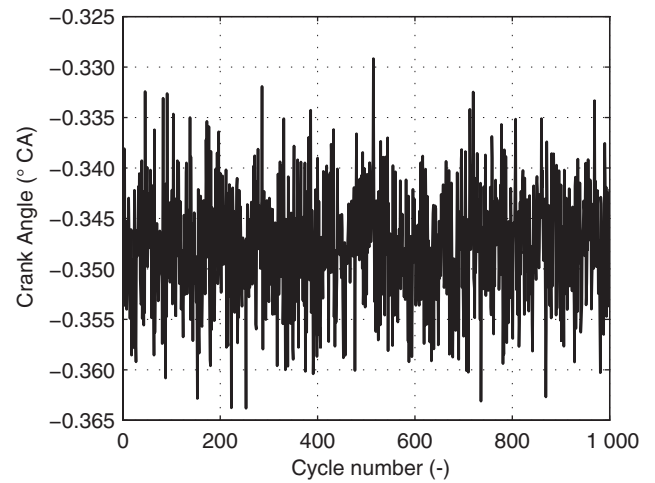


Figure 8

Maximum pressure location extracted from third order Fourier series fits from 1000 simulated motored pressure cycles. Realistic measurement noise with a standard deviation of 2 kPa was added.

ing in internal combustion engines have an unknown bias level that has to be estimated (pegged) somehow. There are various methods for estimating this bias level. One method is to measure the intake pressure and assume that the pressure in the cylinder is equal to the pressure in the intake at some Crank Angle near the bottom dead center during the intake stroke. Another method is to use polytropic pegging during a part of the compression stroke. The quality of the polytropic pegging depends on correct Crank Angle phasing which is not available at the time of pegging. Thus, an approximate TDC location based on the location of maximum pressure is used. Forcing the location of the maximum pressure to somewhere in the range $0.3\text{--}0.6^\circ$ CA as explained above normally provides sufficient accuracy.

It is also possible to include the bias level as an additional parameter in Equation (7). The model depends linearly on the bias level which means that the LLS problem would grow to estimation of three parameters whereas the NLLS problem would still be a one-parameter problem. It turns out however that the standard deviation of the TDC offset estimate is about twice as large when including the pressure bias in the model and thus it is favorable to estimate the pressure bias separately as needed.

2.6 Computing the Pressure Derivative in the Presence of Measurement Noise

The most straightforward way to compute the pressure derivative is to use a central finite difference approximation based on the available pressure measurements. Measurement noise is however amplified by numerical differentiation and fluctuations of about $20 \text{ kPa}/^\circ \text{ CA}$ can be seen in

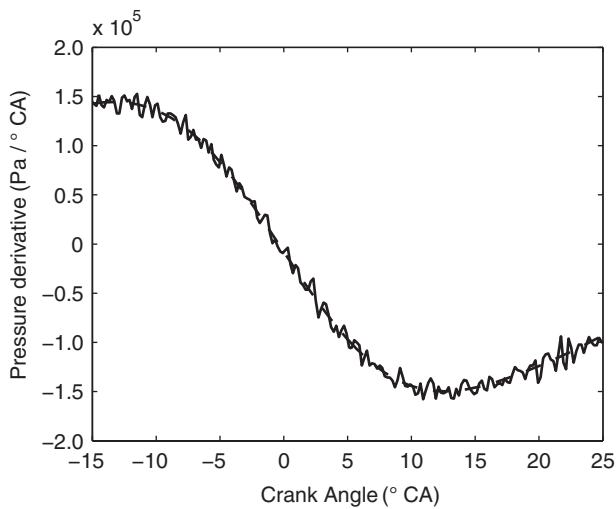


Figure 9

Pressure derivative computed from raw pressure measurements (solid) and from third order Fourier series fit.

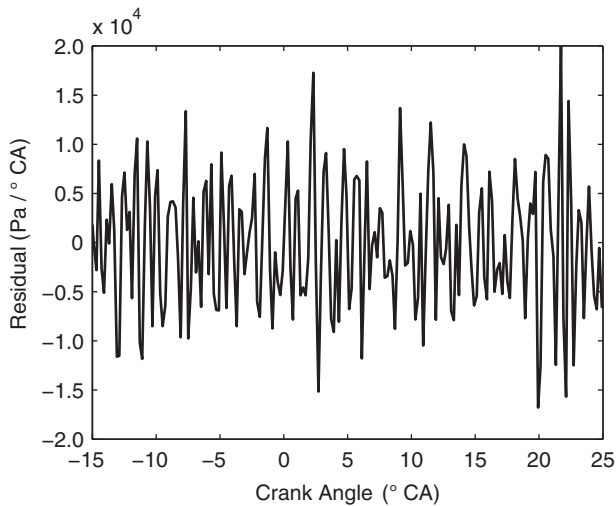


Figure 10

Residuals when replacing the raw pressure derivative with the derivative based on the third order Fourier series fit.

the numerical pressure derivative shown in Figure 9. In the same figure the derivative based on the third order Fourier series approximation mentioned above can also be seen. The pressure derivative based on the Fourier series is noise free and, as can be seen in the figure, picks up the underlying features of the raw pressure derivative very well. Figure 10 shows the residuals when replacing the raw pressure derivative with the derivative based on the Fourier series fit and it is clear that only measurement noise is left in the residuals.

The high quality of the Fourier series cylinder pressure fit and its derivative encourages an attempt to apply them in

the optimization algorithm to find the TDC offset and the specific heat ratio.

3 EXPERIMENTAL SETUP

A Scania DSC12 six-cylinder engine with 12 liter displacement volume is used to evaluate the proposed TDC estimation method. Each cylinder is equipped with Kistler 7061B water-cooled piezoelectric cylinder pressure sensors connected to Kistler 5011B charge amplifiers.

A Kistler 2629B capacitive TDC sensor system is in some cases used as an absolute reference measurement for validation purposes. The relative Crank Angle is measured with a high-resolution encoder from Leine & Linde which produces 1 800 pulses per revolution as well as an index pulse every revolution. Custom made circuitry is used to mask every other index pulse in order to provide a four-stroke reference index. The encoder is adjusted such that the index pulse appears close to Gas Exchange Top Dead Center (GETDC).

4 RESULTS

The proposed TDC estimation method is validated using a Scania DSC12 heavy duty engine against absolute TDC measurements with a capacitive displacement sensor. A test is also performed to see how the TDC estimate is affected by a change in engine speed. Finally an evaluation of the performance with and without use of the Fourier series fit is presented.

It turns out that the difference in average TDC estimates between the method with and without Fourier series fit is negligible and therefore Figures 11–14 are exactly the same as the corresponding figures in [10]. It will however be shown below that there is a significant improvement in estimation variance when applying the Fourier series fit.

4.1 TDC Sensor Validation

Figure 11 shows the 100-cycle average response from the TDC sensor installed in Cylinder 6 with Crank Angle reference determined using the proposed estimation method. It can be seen that the highest amplitude is indeed obtained at Crank Angle zero although the Crank Angle resolution in the measurements is not enough to give better accuracy than about $\pm 0.1^\circ$ CA.

Figure 12 shows a similar validation experiment performed on Cylinder 5. It can be seen here that there is a local minimum in the TDC sensor signal at Crank Angle zero which could be due to measurement noise.

Figure 13 shows a second validation experiment for Cylinder 5, and this time there is indeed maximum amplitude at Crank Angle zero.

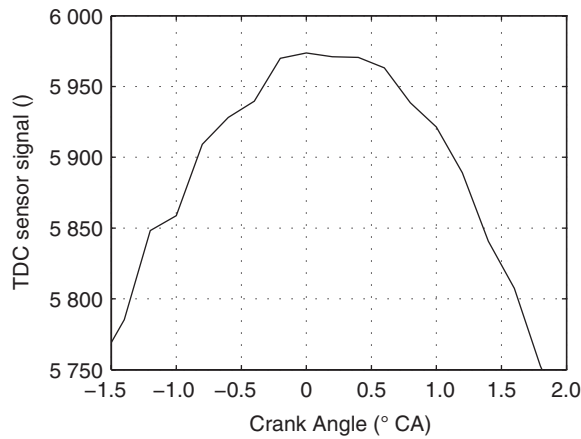


Figure 11
TDC sensor output of cylinder 6 with TDC offset determined from cylinder pressure measurements (not simultaneous measurements).

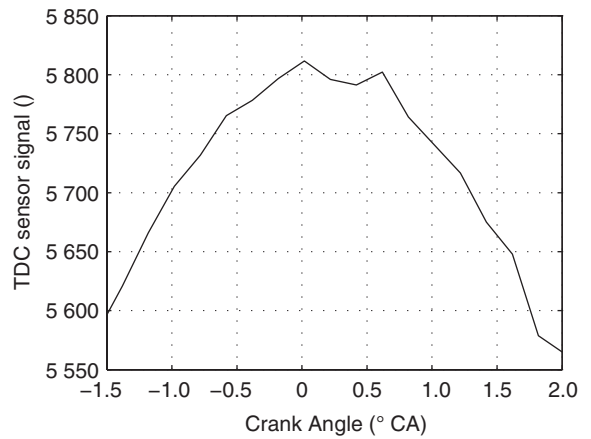


Figure 13
TDC sensor output of cylinder 5 with TDC offset determined from cylinder pressure measurements (not simultaneous measurements).

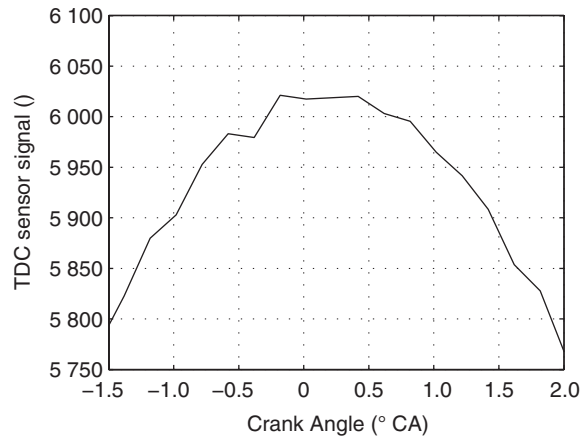


Figure 12
TDC sensor output of cylinder 5 with TDC offset determined from cylinder pressure measurements (not simultaneous measurements).

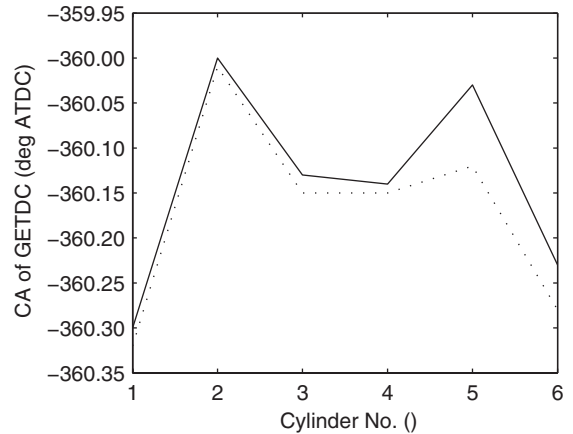


Figure 14
TDC estimates for cylinders 1-6 at 600 (solid) and 1000 (dotted) rpm respectively. 100-cycle averages.

4.2 Engine Speed Dependence

In Figure 14 a comparison between TDC estimates for all six cylinders at two different engine speeds is shown. The diagram actually shows the Crank Angle of the GETDC encoder index pulse, *i.e.* the Crank Angle of the first pressure sample in each cycle, using Crank Angle reference from the proposed estimation method. Four out of six cylinders show differences of 0.02° or less between the two engine speeds. Cylinder 6 shows a difference of 0.05° CA whereas Cylinder 5 shows a difference of 0.09° CA.

Figure 15 shows TDC estimates for 100 consecutive cycles on Cylinder 1 at 600 rpm. It can be seen that all but a few estimates stay within a ±0.1° CA deviation from the average TDC estimate.

4.3 Evaluation of the Third Order Fourier Series Pressure Fit

It has been shown above that a third order Fourier series fit can describe the motored cylinder pressure with very good accuracy. It remains to be shown that it improves the TDC offset estimation though.

A comparison was performed between three different levels of applying the Fourier series cylinder pressure fit:

- no use of Fourier series fit,
- use Fourier series fit to find location of maximum pressure,
- use Fourier series fit both to find maximum pressure location and in the optimization algorithm.

The comparison was performed both for simulated and measured cycles. The simulated cycles, again, had a

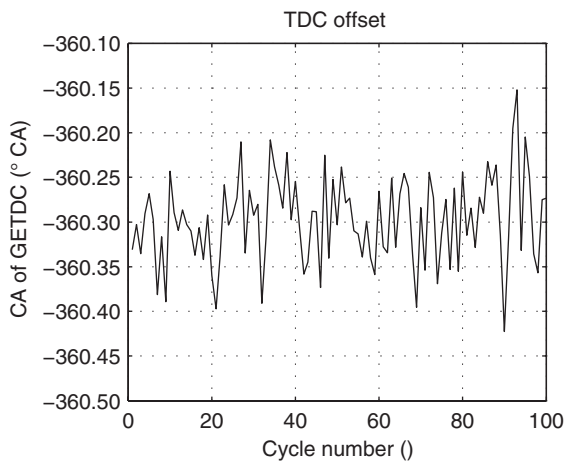


Figure 15

TDC estimates for 100 consecutive cycles of Cylinder 1 at 600 rpm.

measurement noise level of 2 kPa. The measured cycles consisted of a total of 100 pressure cycles each from 6 cylinders at 600 rpm engine speed and the same number of pressure cycles at 1 000 rpm engine speed. This makes a total of 1 200 measured pressure cycles. No significant difference in the standard deviation of the TDC estimates could be found between different engine speeds and different cylinders and therefore the average standard deviation for each level of Fourier series application is also presented. The detailed result of the comparison is presented in Table 1 and the average result is shown in Figure 16.

TABLE 1

Detailed comparison of TDC estimate standard deviations for simulated as well as measured pressure cycles. The standard deviation for each cylinder at each engine speed is computed from 100 measured pressure cycles

Type	Cycles	Level 1	Level 2	Level 3
Simulated		0.0268	0.0203	0.0188
600 rpm	1	0.0303	0.0260	0.0205
600 rpm	2	0.0338	0.0317	0.0205
600 rpm	3	0.0287	0.0295	0.0224
600 rpm	4	0.0314	0.0330	0.0244
600 rpm	5	0.0323	0.0311	0.0217
600 rpm	6	0.0335	0.0327	0.0222
1 000 rpm	1	0.0298	0.0302	0.0241
1 000 rpm	2	0.0290	0.0292	0.0218
1 000 rpm	3	0.0253	0.0241	0.0202
1 000 rpm	4	0.0299	0.0280	0.0202
1 000 rpm	5	0.0320	0.0329	0.0231
1 000 rpm	6	0.0290	0.0349	0.0232

From the comparison it was concluded that the improvement in standard deviation for measured cycles when

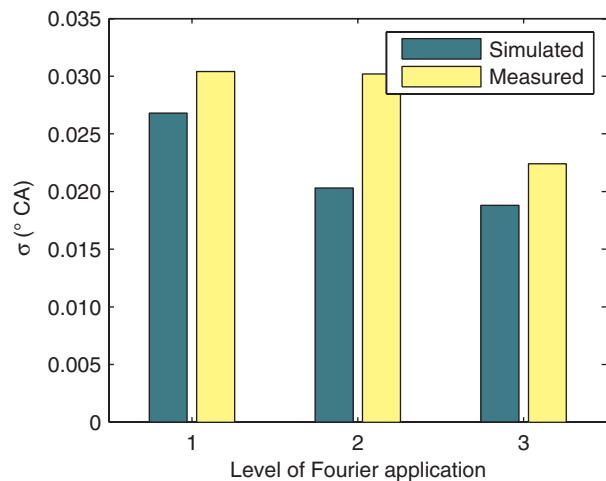


Figure 16

Comparison between standard deviations with different levels of Fourier series application for TDC estimation. Level 1: no use of Fourier series, Level 2: Fourier series for maximum pressure location, Level 3: Fourier series for maximum pressure location and optimization algorithm.

using the Fourier series fit for maximum pressure location (Level 2) is insignificant. When also applying the Fourier series fit for the optimization algorithm (Level 3) the improvement is as much as 26% however. For simulated cycles the improvement from applying Level 2 is 7% whereas the improvement from applying Level 3 (compared to Level 1) is 30%.

5 DISCUSSION

Although the accuracy of the TDC estimate is good for all six cylinders it seems like Cylinders 5 and 6 are less accurate than Cylinders 1-4, not in terms of increased standard deviation of the estimate but in terms of dependence on engine speed. This could be due to a longer distance to the Crank Angle encoder and thus more influence from elastic dynamics in the crank shaft. If the torsional dynamics lead to elastic vibrations with a similar frequency as the engine speed this could lead to changing TDC angles from cycle to cycle and thus an increased variance in the TDC estimate. If the dynamics cause vibrations that are significantly faster than the engine speed this could lead to inaccuracies in the thermodynamic model used for the TDC estimation and thus biased estimates.

The method assumes constant heat loss power over the estimation interval. Since the estimation takes place over a Crank Angle interval of merely 36° CA, or 1-4 ms during normal engine operation, the assumption of constant heat losses is valid even for transients, such as fuel cut-off or engine switch-off, since wall heat dynamics are very slow as

shown in [13]. Furthermore the biggest temperature swing over the estimation interval is about 250 K which corresponds to a variation in specific heat ratio by merely two percent. The same argument holds also with respect to the relatively fast engine speed transients that result from particularly engine switch-off. A reasonable engine deceleration for such a case would be $1\,000\text{ r/s}^2$ which over 4 ms means an engine speed change of 4 r/s or 0.4%. During fuel cut-off the transmission is normally engaged which means that the entire inertia of the vehicle slows down the transient quite significantly.

The model relies on accurate Crank Angle measurements which is not a problem to obtain in a laboratory environment. With production crank sensors the resolution may be as poor as 10° CA, though, which could pose a problem. From the reasoning above, engine speed changes during the estimation interval should be below 0.4% however, which allows accurate Crank Angle interpolation.

The method assumes negligible mass loss during the estimation interval which is of course not entirely true. Mass loss will however be interpreted as heat transfer by the model and as long as the mass loss is small and reasonably constant during the estimation interval it will pose no problem to the estimator. Another related problem arises during motored operation with fuel injection in which case fuel evaporation would affect the cylinder pressure evolution. Again, this would be interpreted as heat transfer by the model and given that the evaporative cooling is sufficiently constant during the estimation it would not affect the quality of the estimate.

The assumption of no chemical reactions is normally quite valid for motored operation. The temperature stays below approximately 1 000 K independent of engine type which means that equilibrium reactions are slow enough to assume frozen composition. If the model were to be applied for fired cycles the estimation interval would most likely have to be modified in order to avoid chemical reactions during the estimation. This would most likely introduce a significant bias in the estimate but could nevertheless be possible.

There is an apparent difference in improvement from applying the third order Fourier series fit between simulated and measured cycles. The simulated cycles show a significant improvement just from applying the Fourier fit for finding the maximum pressure location and then even more improvement when also applying the Fourier fit in the optimization algorithm. For measured cycles there is no improvement from just applying the Fourier fit for finding the maximum pressure location but instead the whole improvement appears when applying it also in the optimization algorithm. The reason for this difference is unknown but could perhaps be caused by dynamics in the crank mechanism that are not taken into account by the simple crank mechanism applied in this study.

The computational time of the Fourier series fit is not negligible but increases the estimation time per cycle from about 16 ms to 57 ms when implemented in Matlab on a personal computer. Although DSP capability may decrease the difference it will most likely still be significant. It should however be kept in mind that TDC estimation is not something that will have to be performed every cycle during the operation of the engine but only on the relatively rare occasions when there is no combustion *i.e.* during startup or fuel cut-off.

CONCLUSION

A new method to accurately estimate the TDC location for an internal combustion engine cylinder based on cylinder pressure measurement has been developed. The method relies on a simple thermodynamic model of the gas inside the combustion chamber including both work and heat interaction. The major assumption made in the model is that the heat losses are constant during the Crank Angle interval used for estimation. Three parameters are estimated by the model; a heat loss constant, the specific heat ratio and the TDC offset. The nonlinear three-parameter least squares problem is separated into a linear least squares problem with two parameters and a nonlinear least squares problem with one parameter which is solved iteratively.

The standard deviation of a single-cycle TDC offset estimate is approximately 0.025° CA with the selected crank encoder resolution of 1 800 pulses per revolution. The bias is approximately 0.01° CA. The TDC estimates are correct to within measurement accuracy when compared to a capacitive displacement TDC sensor. The estimates are also consistent when performed at different engine speeds. Replacing the raw cylinder pressure measurements with a third order Fourier series reduces the standard deviation of single-cycle TDC offset estimation by 25-30% for both simulated and measured cycles.

The proposed method can be applied both for calibration purposes and diagnostic purposes. Calibration of TDC offset is important both for production engines with cylinder pressure based control and for accurate cylinder pressure analysis in a laboratory. Diagnostics could be performed on production engines every time an engine is switched off. There is a substantial number of motored cycles before the engine stops completely when an engine is switched off. Other opportunities for diagnostics is during cranking or during fuel cut-off when engine braking.

REFERENCES

- 1 Brunt M.F.J., Emtage A.L. (1996) Evaluation of IMEP routines and analysis errors, *SAE Technical paper* 960609.
- 2 Heywood J.B. (1988) *Internal Combustion Engine Fundamentals*, McGraw-Hill, pp. 384-385.

- 3 Tazerout M., Le Corre O., Rousseau S. (1999) TDC determination in IC engines based on the thermodynamic analysis of the temperature-entropy diagram, *SAE Technical paper* 1999-01-1489.
- 4 Stas M.J. (1996) Thermodynamic determination of T.D.C. in piston combustion engines, *SAE Technical paper* 960610.
- 5 Stas M.J. (200) An universally applicable thermodynamic method for T.D.C. determination, *SAE Technical paper* 2000-01-0561.
- 6 Eriksson L. (1998) Requirements for and a systematic method for identifying heat-release model parameters, *SAE Technical paper* 980626.
- 7 Xi-Bo Wang, Kang-Yao Deng, Fang-Zheng He, Zhen-Hua Zhou (2007) A thermodynamics model for the compression and expansion process during the engine's motoring and a new method for the determination of TDC with simulation technique, *Appl. Therm. Eng.* **27**, 11-12, 2003-2010.
- 8 Nilsson Y., Eriksson L. (2004) Determining TDC position using symmetry and other methods, *SAE Technical paper* 2004-01-1458.
- 9 Chang H., Zhang Y., Chen L. (2005) An applied thermodynamic method for correction of TDC in the indicator diagram and its experimental confirmation, *Appl. Therm. Eng.* **25**, 5-6, 759-768.
- 10 Tunestål P. (2009) Model Based TDC Offset Estimation from Motored Cylinder Pressure Data, *2009 IFAC Workshop on Engine and Powertrain Control, Simulation and Modeling*, 2008.
- 11 Tunestål P. (2009) Self-tuning gross heat release computation for internal combustion engines, *Control Eng. Pract.*, **17**, 4, 518-524.
- 12 Tunestål P. (2001) Estimation of the In-Cylinder Air/Fuel Ratio of an Internal Combustion Engine by the Use of Pressure Sensors, *PhD Thesis*, Lund University, Faculty of Engineering.
- 13 Wilhelmsson C., Vressner A., Tunestål P., Johansson B., Särner G., Aldén M. (2005) Combustion chamber wall temperature measurement and modeling during transient HCCI operation, *SAE Technical paper* 2005-01-3731.

*Final manuscript received in June 2011
Published online in October 2011*

Copyright © 2011 IFP Energies nouvelles

Permission to make digital or hard copies of part or all of this work for personal or classroom use is granted without fee provided that copies are not made or distributed for profit or commercial advantage and that copies bear this notice and the full citation on the first page. Copyrights for components of this work owned by others than IFP Energies nouvelles must be honored. Abstracting with credit is permitted. To copy otherwise, to republish, to post on servers, or to redistribute to lists, requires prior specific permission and/or a fee: Request permission from Information Mission, IFP Energies nouvelles, fax. +33 1 47 52 70 96, or revueogst@ifpen.fr.